Supporting Information

Synthetic design of active and stable bimetallic PtTi nanoparticle electrocatalysts for efficient oxygen reduction at fuel cell cathodes

Antonia Herzog[1+], Stefanie Kühl[1#], Jiasheng Lu[1], Raffaele Amitrano[1], Sören Selve[2], Johannes Schmidt[3], Thomas Merzdorf[1], Peter Strasser[1*]

[1]Department of Chemistry, Chemical Engineering Division, Technical University Berlin, 10623 Berlin, Germany

[2]Center for Electron Microscopy (ZELMI), Technical University Berlin, 10623 Berlin, Germany

[3]Department of Chemistry, Functional Materials, Technical University Berlin, 10623 Berlin, Germany

*Email: pstrasser@tu-berlin.de

[#]current address: Department of Interface Science, Fritz-Haber Institut der Max Planck Gesellschaft, Faradayweg 4-6, 14195 Berlin

[+]current address: Research Laboratory of Electronics, Massachusetts Institute of Technology, Cambridge, MA, 02139, USA

Table of Content:

- **Table S1** and **S3** giving compositional information in dependence of annealing and Ti adjustment
- **Table S2**, **S4** and **S5** presenting structural parameters of Rietveld refinement
- **Table S6** and **S7** with additional electrochemical data before and after stability test
- **Figure S1-S16** showing additional characterization of the catalysts from XRD, Rietveld refinement, microscopy, and XPS analysis as well as a PtTi phase diagram
- **Figure S17-S20** depicting electrochemical characterization and correlating structural data before and after stability test
- **Figure S21-S25** presenting GIXRD setup, as well as GIXRD, XPS, and microscopy analysis after electrochemical stability tests

1. ICP-OES – Pt loading and constant PtTi composition upon annealing

Table S1. *Pt weight loading and PtTi composition in dependence of reductive annealing temperature compared to Pt/C catalysts obtained by ICP-OES measurements.*

Sample	Pt loading [wt%]	Ti loading [wt%]	Pt content [at%]	Ti content [at%]
PtTi/C-430°C	22	9	39	61
PtTi/C-700°C	24	8	42	58
PtTi/C-800°C	26	8	43	57
Pt/C	24	0	100	0
Pt/C-700°C	32	0	100	0

The PtTi/C-700°C catalyst showed a Pt metal loading of 24 wt% and a Ti metal loading of 8 wt%. This corresponds to the molar fractions of 42 at% Pt and 58 at% Ti, thus indicating a small excess of Ti in the composition of PtTi/C-700°C. During wet impregnation, Ti was used with an excess of 90 at% Ti of the Ti precursor compared to 10 at% Pt of Pt/C. Accordingly, only a fraction of the Ti amount was coated on and annealed in the Pt/C catalyst and the excess was washed out after wet impregnation. Compared to the as-received Pt/C catalyst with a Pt loading of 24 wt%, the Pt loading of PtTi/C-430°C was slightly reduced to 22 wt%. This corresponds to the additional weight fraction of Ti. Additionally, it could also be influenced by a relative effect of the total mass of the catalyst powders due to a distortion with additional oxygen of remaining TiO_x, as the evaluation assumes pure Pt-Ti on carbon support. Accordingly, in case of unreduced TiO_x the oxygen is neglected in the catalyst mass, and thus, would result in a lower apparent Pt (and Ti) loading. However, this would not affect the relative Pt to Ti content. Moreover, Pt/C annealed at 700°C possesses a higher weight loading of 32 wt% Pt. The reason for this might be a slight decomposition of the support material (Carbon Black) during the thermal annealing process, which would yield in a higher loading of Pt compared to the support. This would also explain the higher Pt loading of 26 wt% in PtTi/C-800°C.

2. XRD evaluation upon annealing

Structural investigation before and after annealing

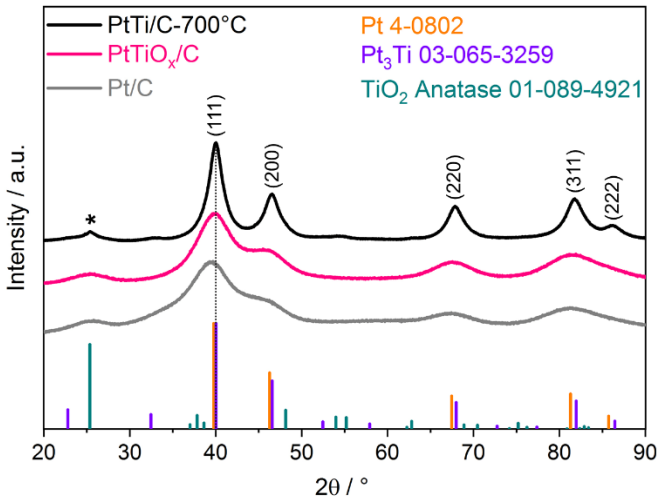

Figure S1. *XRD patterns of as-received Pt/C and PtTiO$_x$/C before thermal annealing and PtTi/C-700°C after thermal annealing. The reference diffraction patterns of the different crystal structures are displayed as colored bars in the bottom. The indices of the crystal planes correspond to the Pt phase and * denotes the (002) plane of graphitic carbon from the support. The dotted line at the (111) reflections illustrates the shift between the patterns.*

3. Increase of particle size of as-received Pt/C catalyst at 700 °C

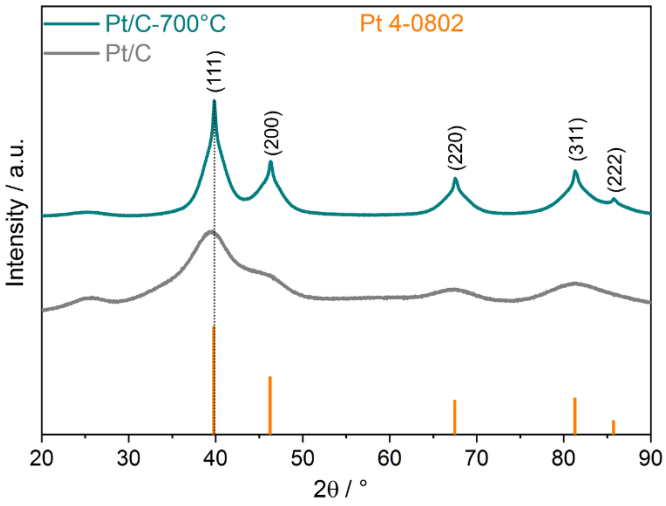

Figure S2. *XRD patterns of Pt/C before and after thermal annealing at 700 °C. The reference diffraction pattern of Pt fcc is displayed as orange bars in the bottom. The dotted line at the (111) reflection illustrates no shift between the patterns.*

Table S2. *Development of crystallite sizes before and after annealing of Pt/C obtained from Rietveld refinement with deducted graphite phase of the XRD pattern.*

Sample	Phase	Fraction [wt%]	Crystallite size (LVolB) [nm][1]
Pt/C	Pt fcc	100	1.05 ± 0.03
Pt/C-700°C	Pt fcc (1)	96 ± 1	2.17 ± 0.01
	Pt fcc (2)	4.2 ± 0.1	26.5 ± 0.4

4. Rietveld refinement – structural parameters upon annealing

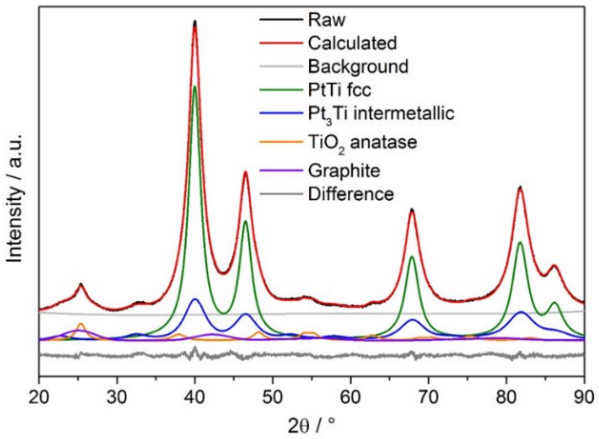

Figure S3. *Exemplary Rietveld refinement of PtTi/C-700°C. The performed calculation shows only small turning points in the difference curve and is therefore regarded as reliable.*

Table S3. *Structural parameters of PtTi/C catalysts upon annealing compared to Pt/C obtained by Rietveld refinement of XRD patterns – weight fractions are given with deducted graphite phase.*

Sample	Phase / Space group	Fraction [wt%]	Crystallite size (LVolB) [nm][1]	Lattice constant [Å]
Pt/C	Pt fcc / Fm3m	100	1.05 ± 0.03	3.93 ± 0.03
PtTi/C-430°C	PtTi fcc / Fm3m	74.5 ± 0.8	1.65 ± 0.02	3.91 ± 0.01
	TiO_2 anatase / I41amd	26.5 ± 0.9	3.7 ± 0.1	3.77 ± 0.01 9.41 ± 0.03
PtTi/C-700°C	PtTi fcc / Fm3m	48.5 ± 0.8	3.31 ± 0.05	3.895 ± 0.004
	Pt_3Ti ordered / Pm-3m	20.3 ± 0.8	2.16 ± 0.08	3.891 ± 0.004
	TiO_2 anatase / I41amd	31.2 ± 0.9	4.1 ± 0.1	3.767 ± 0.004 9.47 ± 0.01
PtTi/C-800°C	PtTi fcc / Fm3m	32 ± 1	3.36 ± 0.03	3.896 ± 0.004
	Pt_3Ti ordered / Pm-3m	33 ± 3	5.26 ± 0.05	3.889 ± 0.004
	TiO_2 anatase / I41amd	35 ± 2	3.5 ± 0.1	3.773 ± 0.005 9.47 ± 0.01

5. Binary Ti–Pt phase diagram

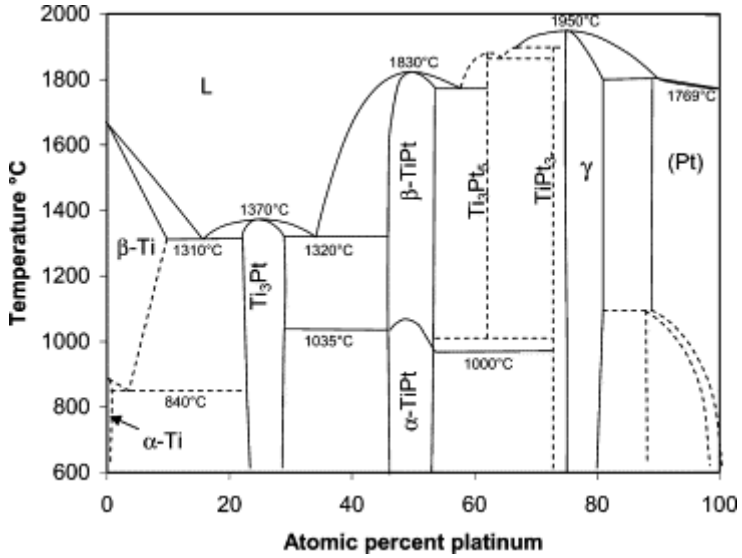

Figure S4. *Ti–Pt phase diagram after Murray et al.[2] The macroscopic thermodynamic stable phase diagram for the PtTi system contains three intermetallic phases: $PtTi_3$, PtTi and Pt_3Ti. When the Pt at% is in the range between 65-75 %, the PtTi phase forms at lower temperatures between 600-1000 °C, whereas the Pt_3Ti phase forms at higher temperatures between 1000-1900 °C. The lower annealing temperatures needed in our experiments to form Pt_3Ti may result from reductive transformation of Pt and TiO_x as well as different behavior for nanoparticles that can enhance reactivity and lower the energy barriers for phase transformations.*

6. TEM particle size distribution upon annealing

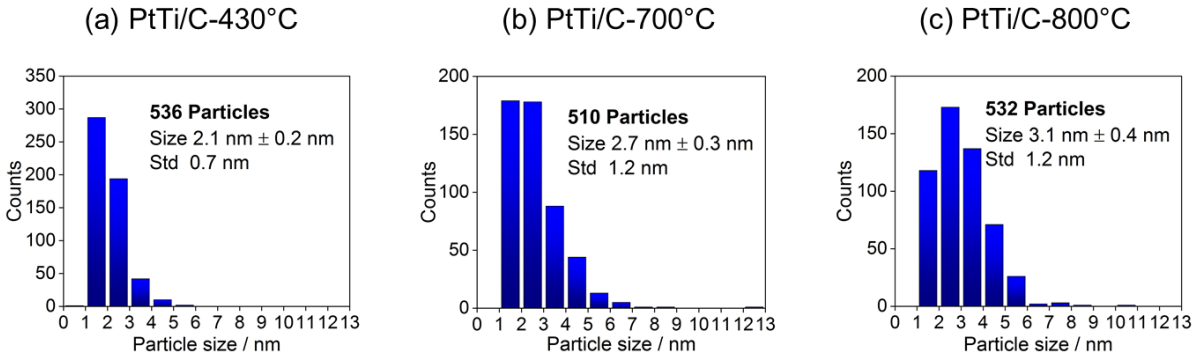

Figure S5. *Particle size distributions determined from TEM images – for every sample over 500 particles were measured. The average of the particle diameters is given with a calculated error, and the standard deviation (Std) of the mean is noted in addition.*

7. TEM micrograph and particle size distribution of as-received catalyst Pt/C

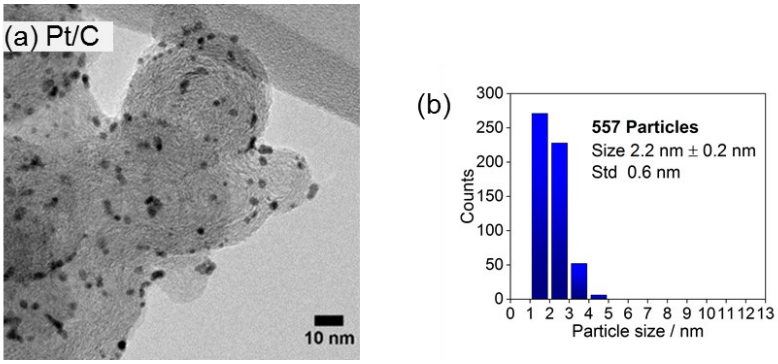

Figure S6. *(a) TEM micrograph of as-received catalyst Pt/C and (b) corresponding particle size distribution. The average of the particle diameters is given with a calculated error, and the standard deviation (Std) of the mean is noted in addition.*

8. STEM and HRTEM analysis of PtTi/C-700°C

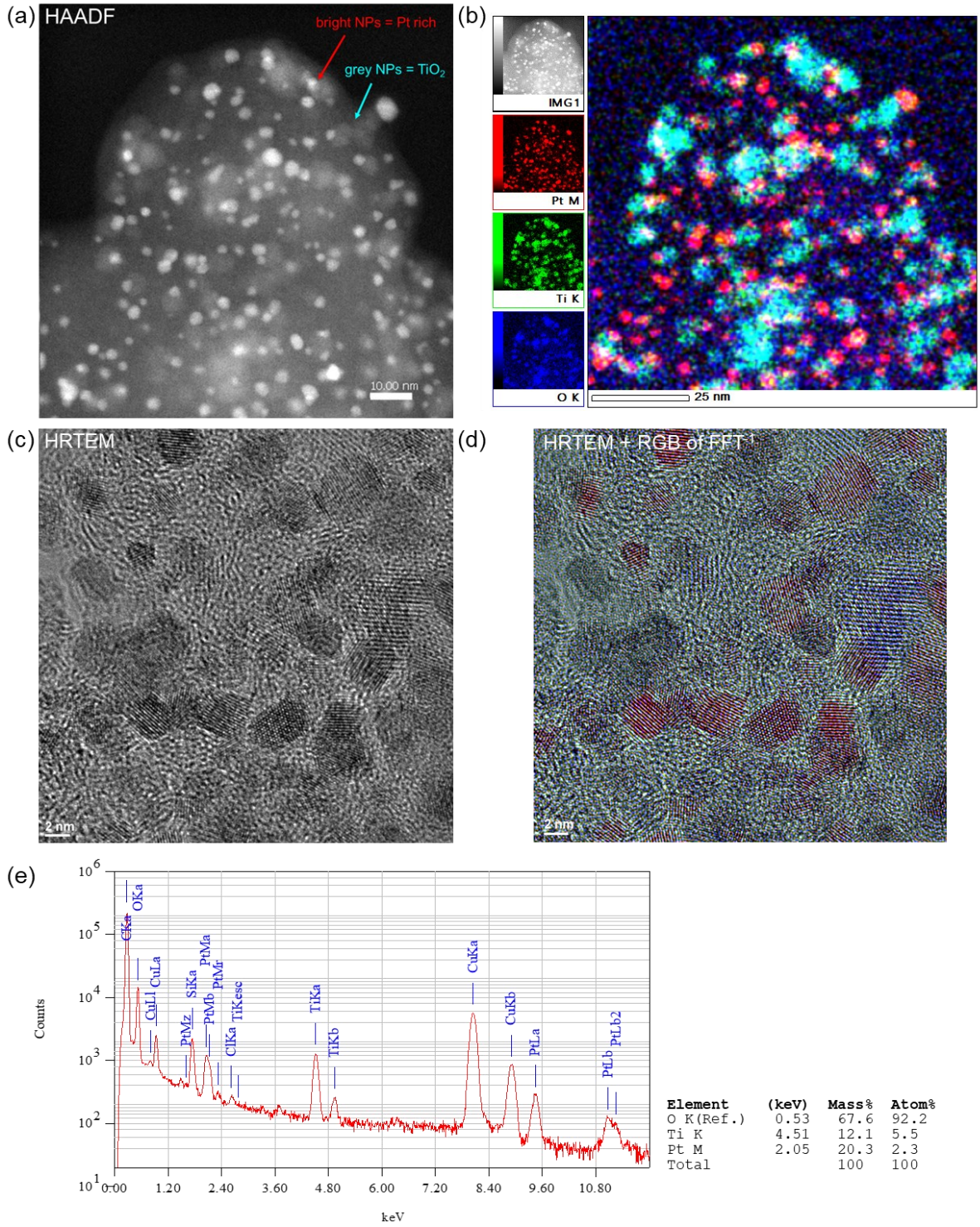

Figure S7. *STEM, EDX and HRTEM images of as-prepared PtTi/C-700°C. (a) STEM-HAADF images, where bright nanoparticles (NPs) represent the Pt(Ti) rich particles and grey NPs TiO_2 particles on the carbon support. (b) EDX mapping of corresponding region in (a) of Pt (red), Ti (green), and O (blue). (c) High resolution TEM (HRTEM) image indicates different lattice planes from the different particles. (d) Overlap of HRTEM and RGB image using the different composition/phases of Pt (red) and TiO_2 (blue) from the inverse fast fourier transforms (FFTs) obtained by the sum of all filtered FFTs of the same composition/phase. (e) EDX spectrum with quantification from whole area in (a) and (b).*

9. HRTEM and FFT analysis of PtTi/C-700°C

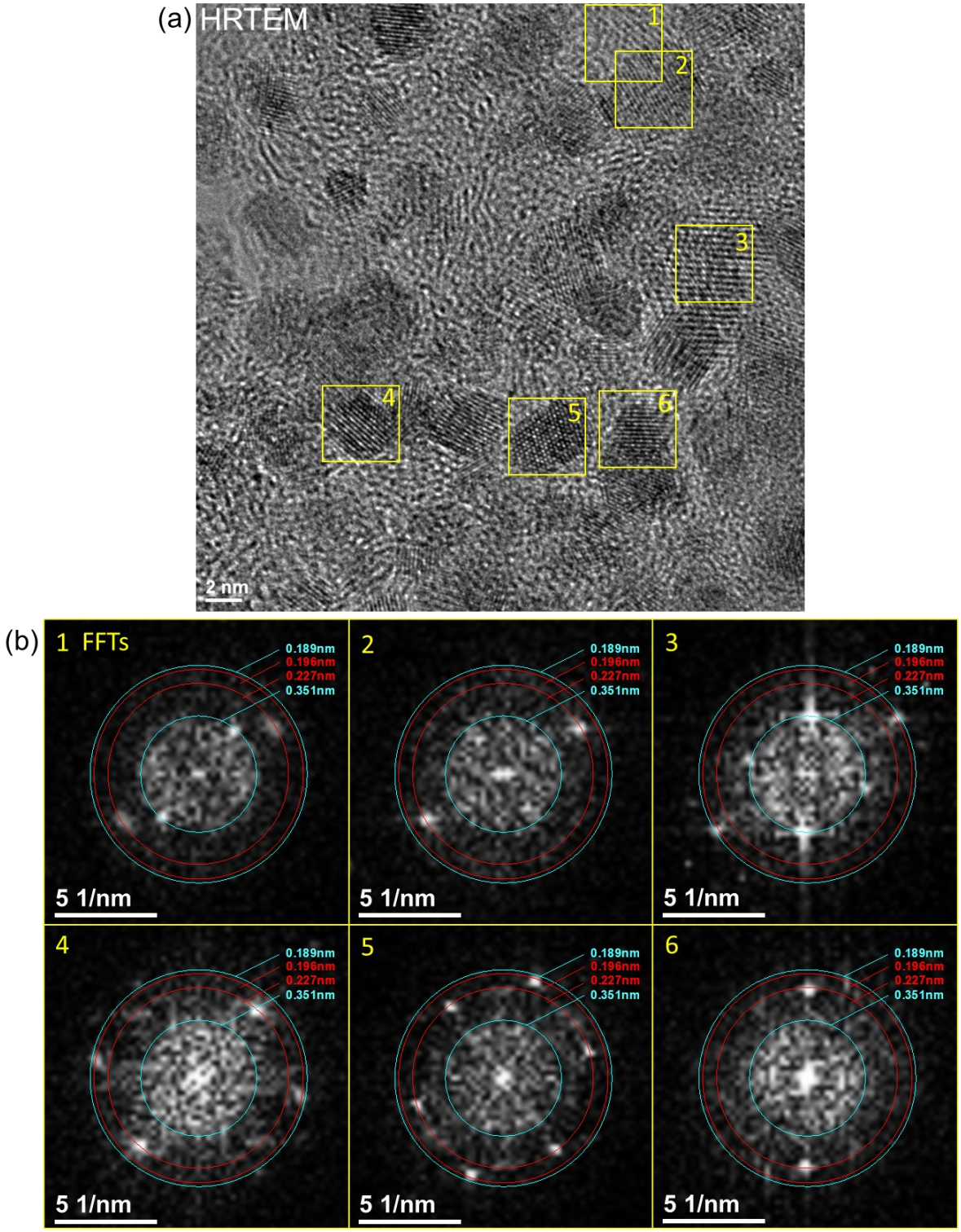

Figure S8. *(a) HRTEM image with selected areas used for FFTs. (b) FFTs of selected areas, where reflections on red circles match well with (111) and (200) lattice planes of fcc Pt(Ti) and reflections on blue lines with (101) and (200) lattice planes of* TiO_2 *anatase.*

10. EDX analysis of single particles in PtTi/C-700°C

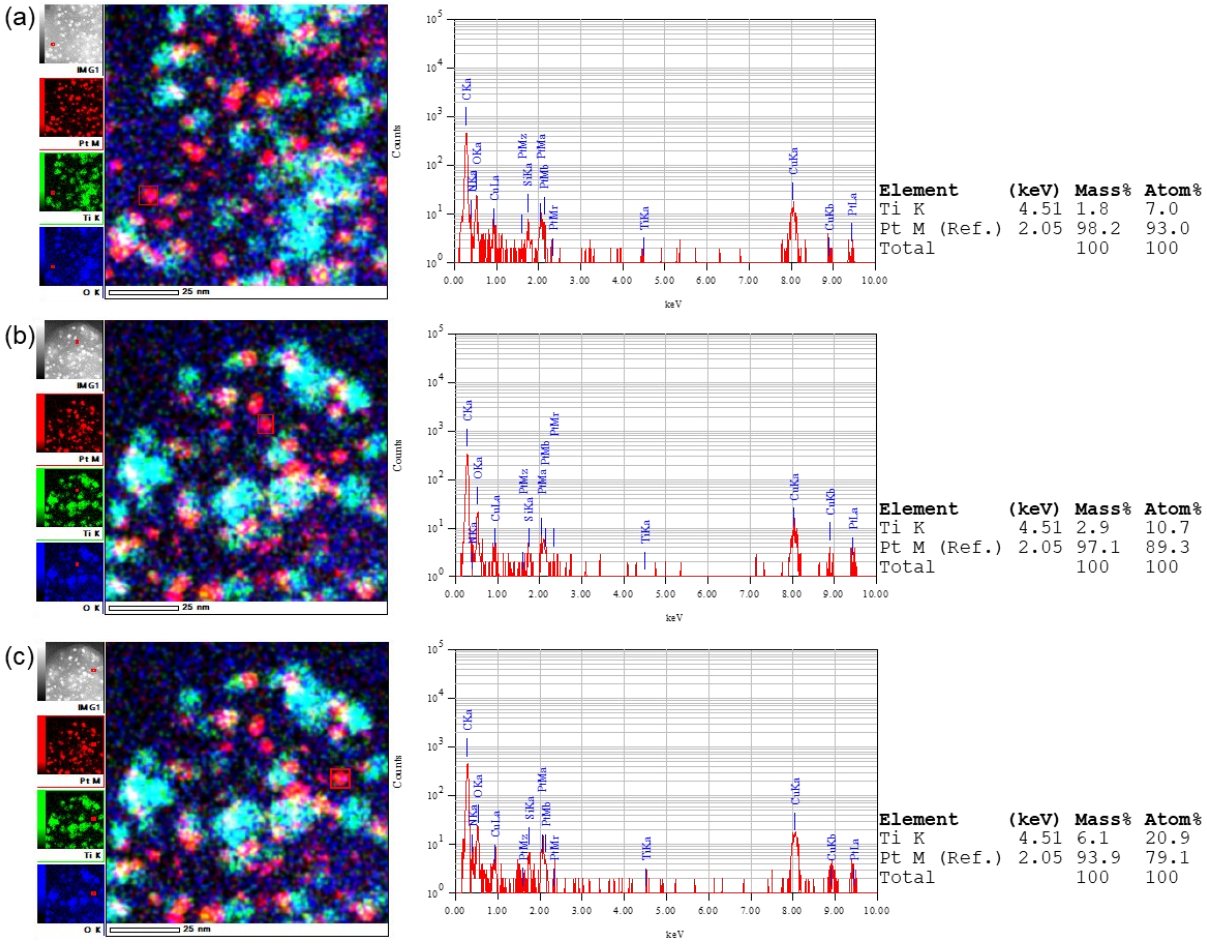

Figure S9. *EDX analysis including mapping, selected particle spectrum, and quantification. These results are exemplified by several particles from the mapping in* ***Figure S7****b. From (a) to (c), the particles display an increasing amount of Ti incorporated into the Pt particles. The EDX analysis confirms the presence of Ti alongside Pt in the particles. It is important to note the measurement uncertainties, such as the small particle size leading to low X-ray yield, limited measurement time due to contamination and beam damage, and the inherent TEM-EDX accuracy of approximately 15% due to the standardless measurement method. Despite these uncertainties, the results indicate a consistent trend, showing the presence of both Pt and Ti in the particles, along with the occurrence of* TiO_2 *particles from* ***Figure S7****e.*

11. Adjustment of Ti content – variation of initial amounts of Ti precursor during impregnation

Table S4. *Initial amounts of Pt in Pt/C and Ti in titanium(IV) butoxide with varied Ti amount in wet impregnation – described as total amounts and molar fractions of the samples.*

Sample	Initial amount of Pt		Initial amount of Ti	
	[mmol]	[at%]	[mmol]	[at%]
PtTi/C-0.5	0.10	18.5	0.44	81.5
PtTi/C-0.65	0.10	14.9	0.57	85.1
PtTi/C-0.75	0.10	13.1	0.66	86.9
PtTi/C-1.0	0.10	10.2	0.88	89.8
PtTi/C-1.5	0.10	7.0	1.33	93.0

12. XRD evaluation upon Ti adjustment

Rietveld refinement – structural parameters upon Ti adjustment

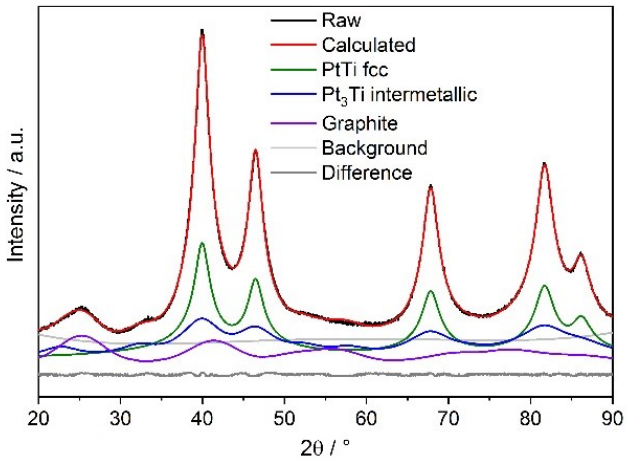

Figure S10. *Exemplary Rietveld refinement of PtTi/C-0.65. The performed calculation shows only small turning points in the difference curve and is therefore regarded as reliable.*

Table S5. *Structural parameters upon Ti adjustment obtained by Rietveld refinement of XRD patterns – weight fractions are given with deducted graphite phase.*

Sample	Phase / Space group	Fraction [wt%]	Crystallite size (LVolB) [nm][1]	Lattice constant [Å]
PtTi/C-0.5	PtTi fcc / Fm3m	73 ± 2	3.93 ± 0.09	3.893 ± 0.004
	Pt_3Ti ordered / Pm-3m	27 ± 2	1.87 ± 0.09	3.899 ± 0.005
PtTi/C-0.65	PtTi fcc / Fm3m	69 ± 1	3.60 ± 0.07	3.896 ± 0.006
	Pt_3Ti ordered / Pm-3m	31 ± 1	1.59 ± 0.08	3.898 ± 0.006
PtTi/C-0.75	PtTi fcc / Fm3m	64 ± 1	3.47 ± 0.06	3.894 ± 0.006
	Pt_3Ti ordered / Pm-3m	23 ± 1	1.7 ± 0.1	3.902 ± 0.006
	TiO_2 anatase / I41amd	13 ± 2	4.3 ± 0.5	3.769 ± 0.007 9.50 ± 0.02
PtTi/C-1.0	PtTi fcc / Fm3m	48.5 ± 0.8	3.31 ± 0.05	3.895 ± 0.004
	Pt_3Ti ordered / Pm-3m	20.3 ± 0.8	2.16 ± 0.08	3.891 ± 0.004
	TiO_2 anatase / I41amd	31.2 ± 0.9	4.1 ± 0.1	3.767 ± 0.004 9.47 ± 0.01

Formation of rutile in PtTi/C-1.5

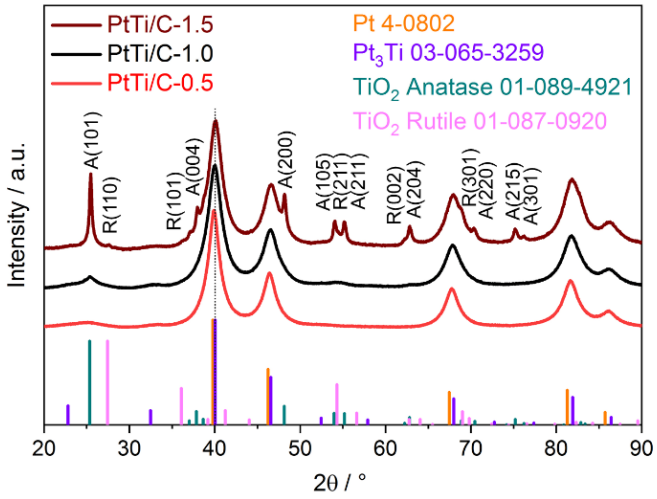

Figure S11. *XRD patterns of PtTi/C catalysts upon initial Ti amount including PtTi/C-1.5, which contains reflections attributed to a rutile phase. The reference diffraction patterns of the different crystal structures are displayed as colored bars in the bottom. The dotted line at the (111) reflection illustrates no shift between the patterns.*

13. XPS analysis of PtTi/C in dependence of the initial Ti amount

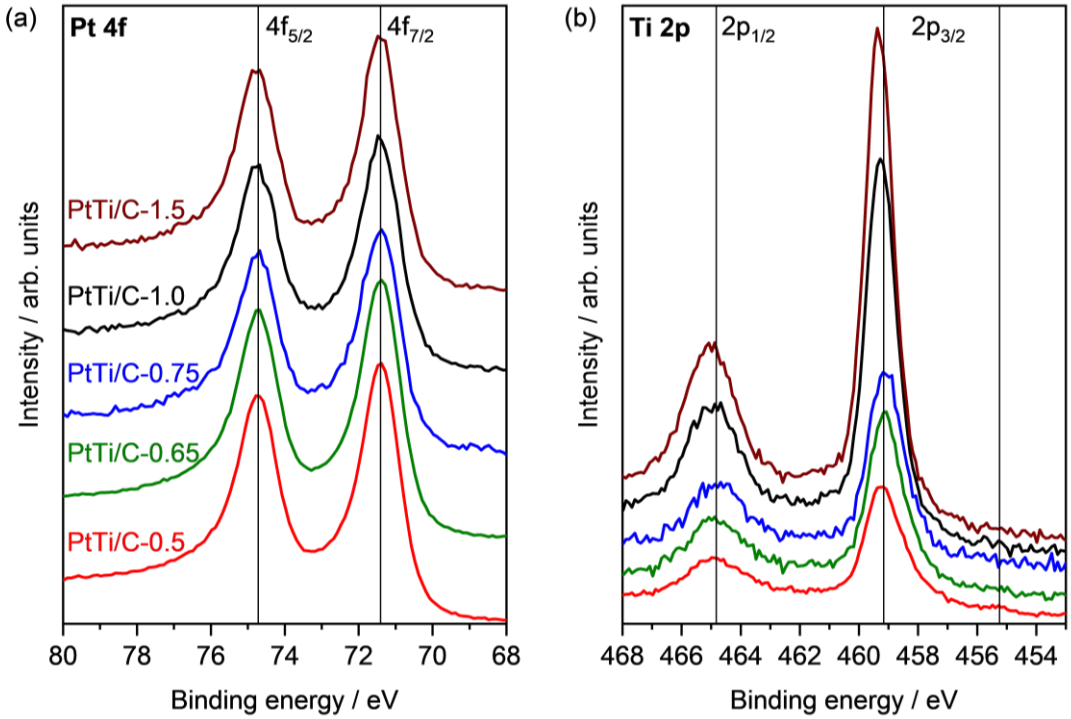

Figure S12. *XPS spectra of PtTi/C catalysts in dependence of the initial Ti amount. (a) Pt 4f and (b) Ti 2p XPS spectra.*

14. TEM micrograph and particle size distribution of adjusted PtTi/C-0.65

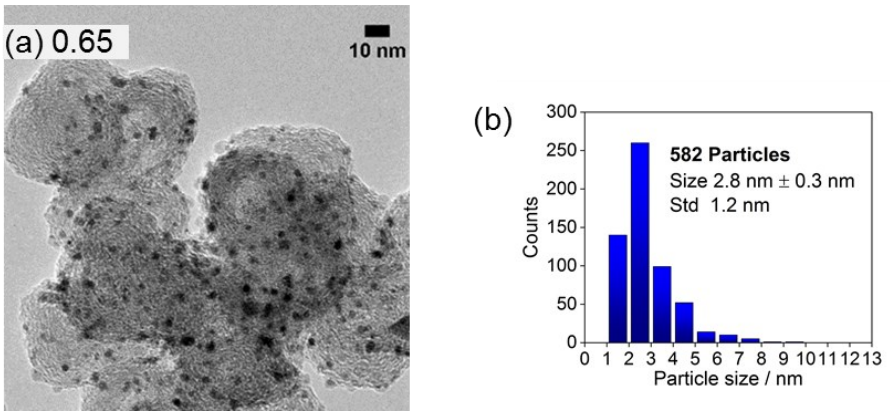

Figure S13. *(a) TEM micrograph of PtTi/C-0.65 with adjusted Ti content and (b) corresponding particle size distribution. The average of the particle diameters is given with a calculated error, and the standard deviation (Std) of the mean is noted in addition.*

15. STEM/EDX analysis of PtTi/C-0.65

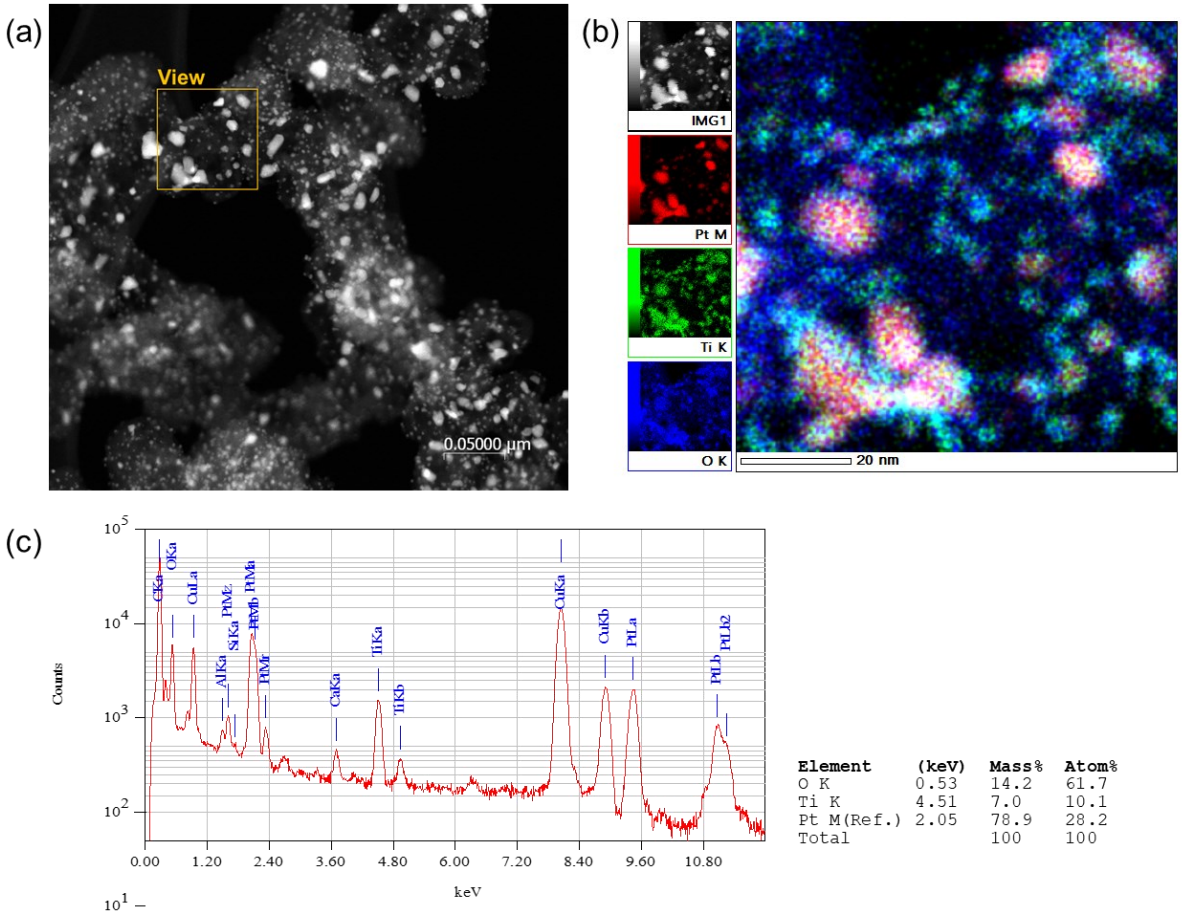

Figure S14. *STEM and EDX* of as-prepared PtTi/C-0.65. *(a) STEM-HAADF image, where bright nanoparticles (NPs) represent the Pt(Ti) particles and grey NPs TiO_2 particles on the carbon support. (b) EDX mapping of corresponding view region in (a) of Pt (red), Ti (green), and O (blue). (c) Corresponding EDX spectrum and quantification from (b).*

16. HRTEM image of PtTi/C-0.65

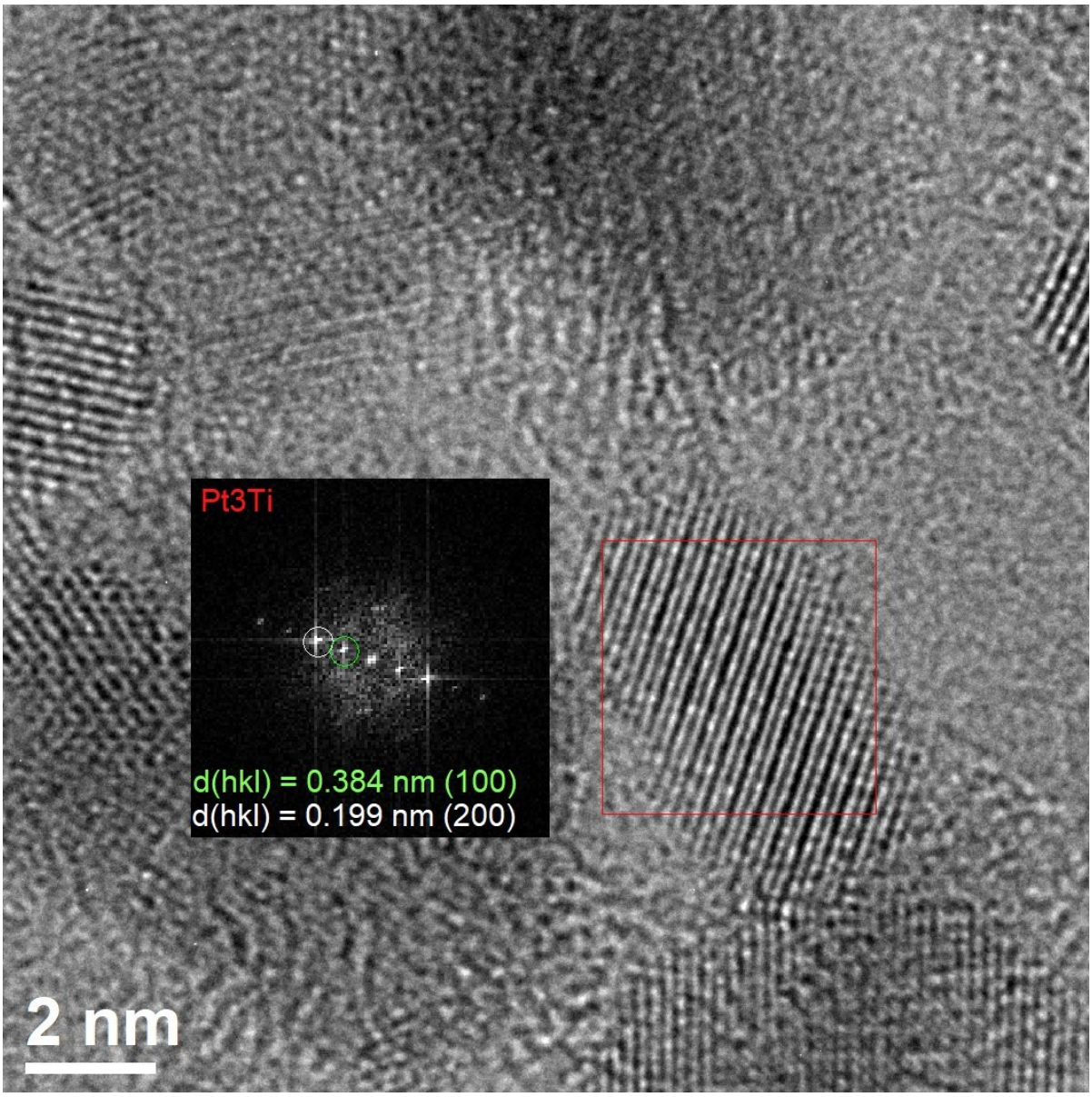

Figure S15. *HRTEM image of PtTi/C-0.65 indicate an overstructure lattice from the intermetallic Pt_3Ti phase with reflections from $Pt_3Ti(100)$ (green) and $Pt_3Ti(200)$ (white).*

17. HRTEM and FFT analysis of PtTi/C-0.65

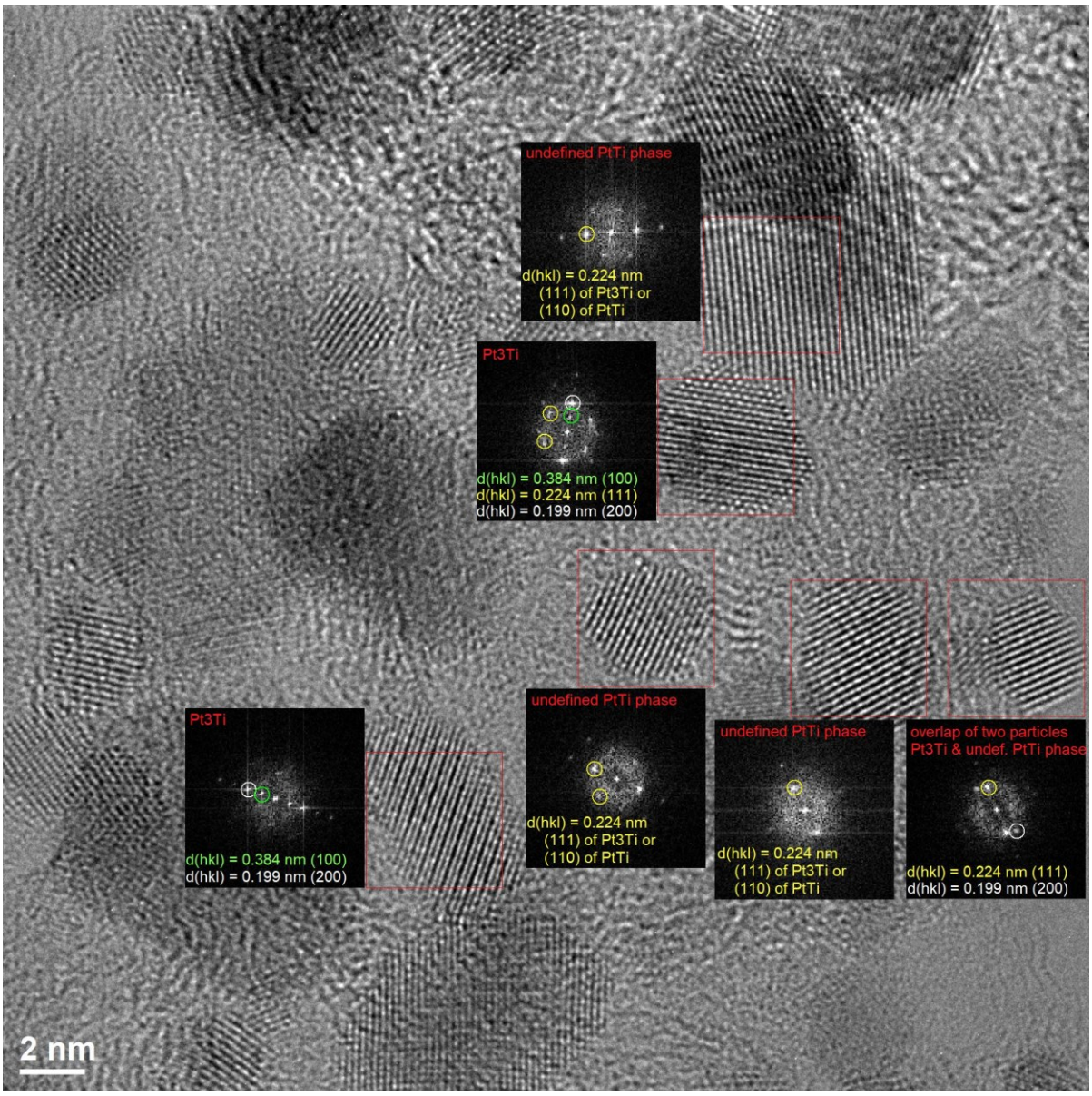

Figure S16. *HRTEM image of PtTi/C-0.65 with FFTs of selected regions, displaying d-spacings of 0.199 nm (white), 0.224 nm (yellow), and 0.384 nm (green), corresponding to reflections from fcc Pt_3Ti and unidentified fcc PtTi phases. For example, the FFT in the bottom-left shows reflections from Pt_3Ti(100) (green) and Pt_3Ti(200) (white). The FFT in the middle displays reflections from Pt_3Ti(100) (green), Pt_3Ti(111) (yellow), and Pt_3Ti(200) (white). The FFT in the bottom-right illustrates the overlap of two particles, where the 0.224 nm reflection (yellow) may correspond to either Pt_3Ti(111) or PtTi(110), while the 0.199 nm reflection (white) is likely from Pt_3Ti(200) in a different particle.*

18. Improvement of electrochemical activity of PtTi/C-1.0 compared to Pt/C catalyst

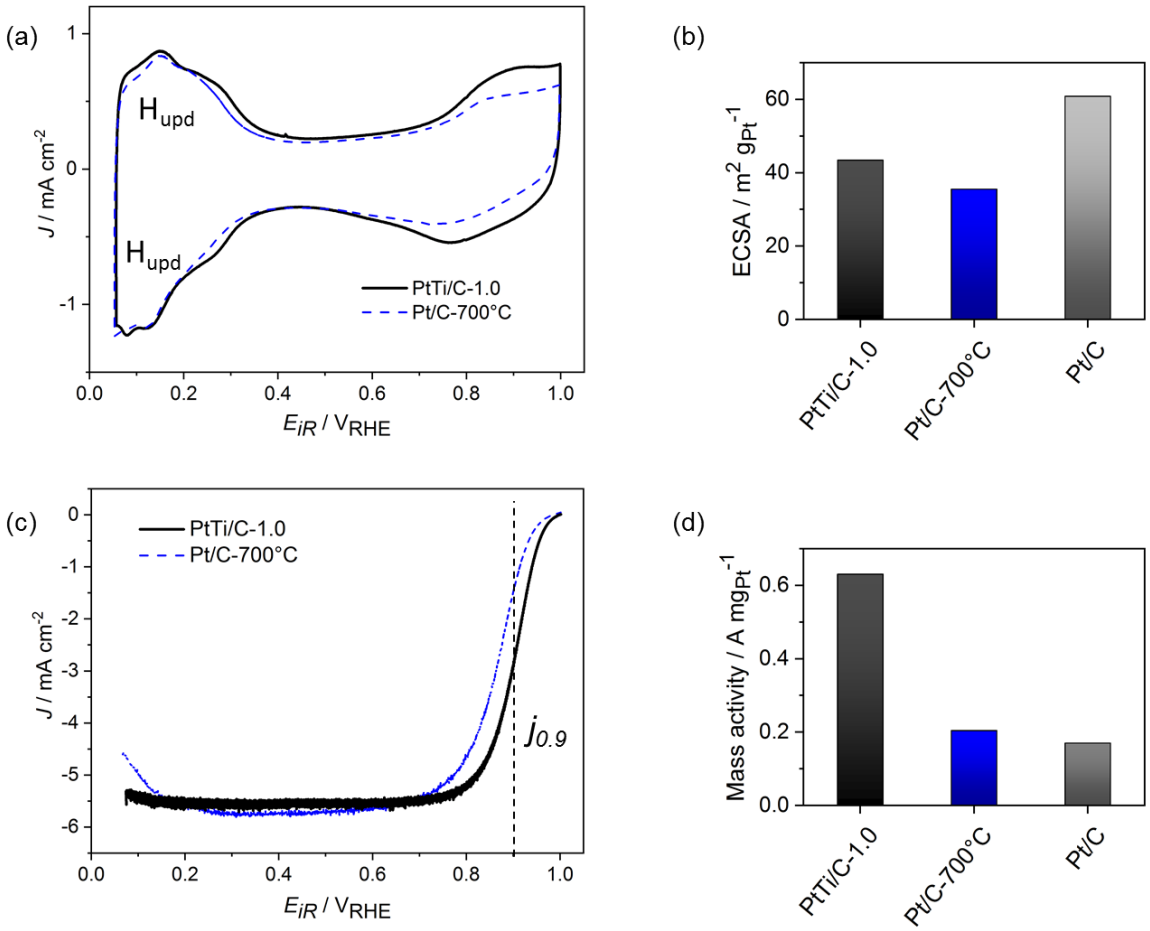

Figure S17. *Electrochemical measurements of PtTi/C-1.0 compared to Pt/C-700°C with an electrode loading of 10 $\mu g_{Pt}/cm^2$: (a) cyclic voltammogram of 25th cycle (measured in N_2-saturated 0.1M $HClO_4$ in the range of +0.05 – +1.00 V_{RHE} with 100 mV s^{-1}), (b) corresponding ECSA based on the H_{upd} region, also compared to Pt/C; (c) linear sweep voltammogram (measured in O_2-saturated 0.1 M $HClO_4$ in the range of +0.05 – +1.00 V_{RHE} with 5 mV s^{-1} and 1600 rpm) and (d) corresponding Pt mass activity, also compared to Pt/C.*

19. ORR performance at different annealing temperatures of PtTi/C-1.0

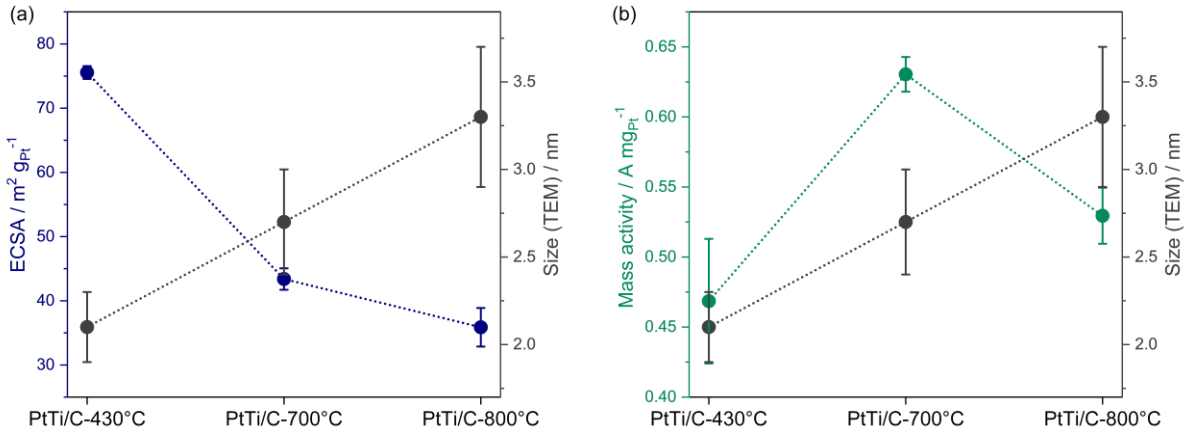

Figure S18. *(a) ECSA and (b) Pt mass activity of PtTi/C-1.0 at different annealing temperatures (430, 700, and 800 °C) correlated to the particle size as determined from TEM analysis (**Figure 4**).*

20. XRD particle size distribution of graphitic carbon at (002) upon annealing

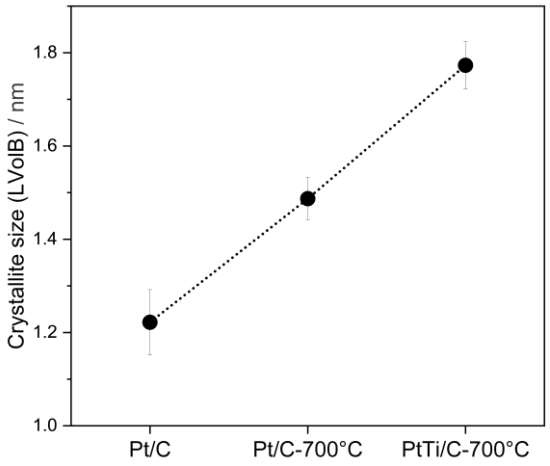

Figure S19. *Crystallite size distribution of graphitic carbon at (002) plane of the Vulcan carbon support of bare Pt/C and PtTi/C at an annealing temperature of 700 °C. The sizes were determined by Rietveld refinement of the corresponding XRD diffractograms.*

21. Reproducibility and Error consideration of electrochemical measurements of PtTi/C

The ECSAs and particularly the activities of the same catalyst after 25 voltage cycles differed sometimes significantly from each other. Several reasons were considered to cause the difference in activity:

(i) Ink consists of an inhomogeneous dispersed catalyst.

(ii) Instability of the prepared ink and/or ink coating on the glassy carbon (GC) electrode.

(iii) Irregular distribution of the ink coating on the GC electrode.

Comment to (i): The catalyst seemed to be well dispersed after ultra-sonification for 30 min. No reprecipitation of particles was observed.

Comment to (ii): To determine the stability of the ink solution and the ink coating on the GC, three electrodes were prepared by coating the ink of PtTi/C-1.0 under different conditions. Electrode 1 (E1) was directly coated with the ink after ink preparation, followed by the immediate measurement of the electrochemical properties. Electrode 2 (E2) was coated with an 1 h old ink, followed by the measurement of the electrochemical properties 3 h after coating. Electrode 3 (E3) was coated with an 5 h old ink, followed by the immediate measurement of the electrochemical properties. **Table S6** lists the three electrodes with the corresponding conditions of coating, ratings of the coating and the obtained ECSAs and mass activities.

Table S6. *Electrodes coated with ink of PtTi/C-1.0 with the corresponding conditions of coating, ratings of the coating and the obtained ECSAs and mass activities.*

Electrode	Age of ink [h]	Age of coating [h]	Rating of coating	ECSA [m^2/g_{Pt}]	Mass activity [A/mg_{Pt}]
E1	0	0	streaks	33.8	0.53
E2	1	3	slight streaks	35.7	0.42
E3	5	0	streaks	31.5	0.36

The Pt mass activity significantly decreased from 0.53 A/mg_{Pt} by using the fresh ink to 0.42 A/mg_{Pt} by using the older ink and electrochemical measurements at a later time, and to 0.36 A/mg_{Pt} by using the even older ink. Consequently, the electrochemical measurements presented in this study were conducted exclusively by using fresh inks for the electrode coating, followed by immediate measurements of the electrochemical properties. In contrast to the decreasing mass activity, the ECSA changed only slightly depending on the distribution of the coating (see rating of coating).

Comment to (iii): Inks of PtTi catalysts were first fabricated with a Pt loading per GC surface area of 10 $\mu g_{Pt}/cm^2$, resulting in an inhomogeneous distribution of the ink coating on the GC. By changing the Pt loading per GC surface area to 15 $\mu g_{Pt}/cm^2$, better distributions of ink coatings on the GC were be obtained.

All in all, several optimizations of the ink preparation and measurement conditions were conducted. However, different electrodes coated with the same catalyst showed sometimes still differences in their electrochemical activity. Hence, the stated electrocatalytic activities in this study are the ones, which were mostly obtained for the respective catalyst out of three to five measurements.

22. Electrochemical stability measurements of PtTi/C-0.65

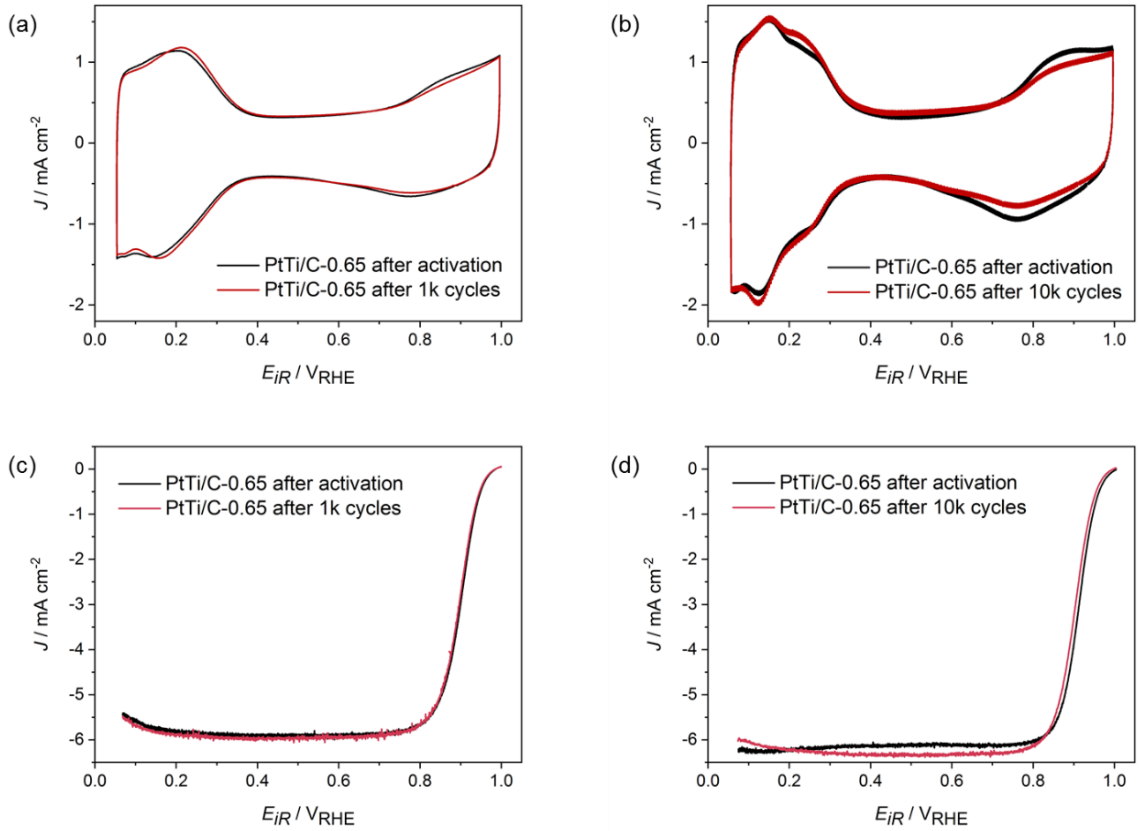

Figure S20. *Stability measurements of PtTi/C-0.65 with an electrode loading of 15 $\mu g_{Pt}/cm^2$: Cyclic voltammograms after (a) 25 and 1k cycles and (b) 25 and 10k cycles (measured in N_2-saturated 0.1 M $HClO_4$ in the range of +0.05 – +1.00 V_{RHE} with 100 mV/s); linear sweep voltammograms after (c) 25 and 1k cycles and (d) 25 and 10k cycles (measured in O_2-saturated 0.1 M $HClO_4$ in the range of +0.05 – +1.00 V_{RHE} with 5 mV/s and 1600 rpm).*

23. GIXRD setup to measure RDE electrode

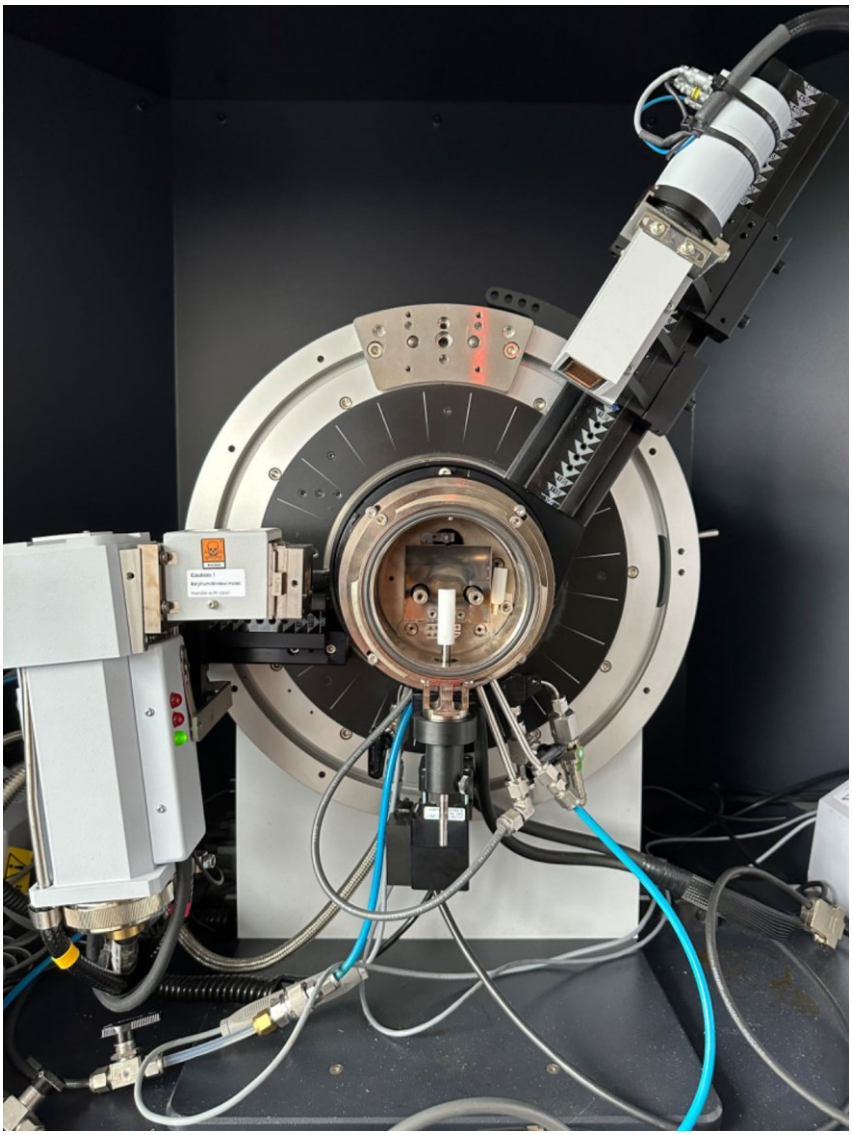

Figure S21. *Picture of the GIXRD setup to measure RDE electrodes before and after electrochemical stability tests.*

24. GIXRD stability measurements of PtTi/C-0.65 on a RDE electrode

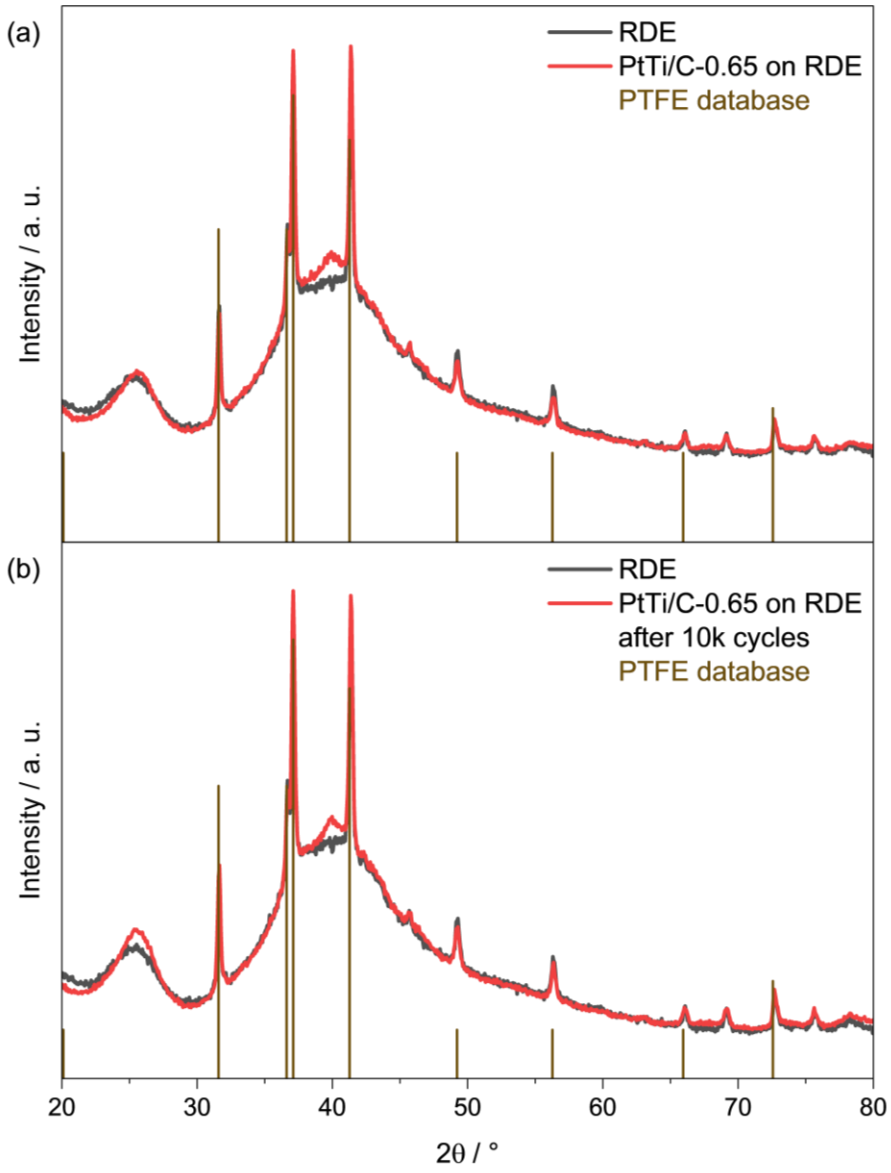

Figure S22. *GIXRD pattern of the RDE and (a) the PtTi/C-0.65 catalyst deposited on the RDE before and (b) after 10,000 cycles AST. PTFE reference is given to account for PTFE from the RDE. Peak at 26.7°2θ belongs to the (002) plane of the glassy carbon from the RDE.*

25. GIXRD stability measurements of PtTi/C-0.65 on a RDE electrode after background subtraction

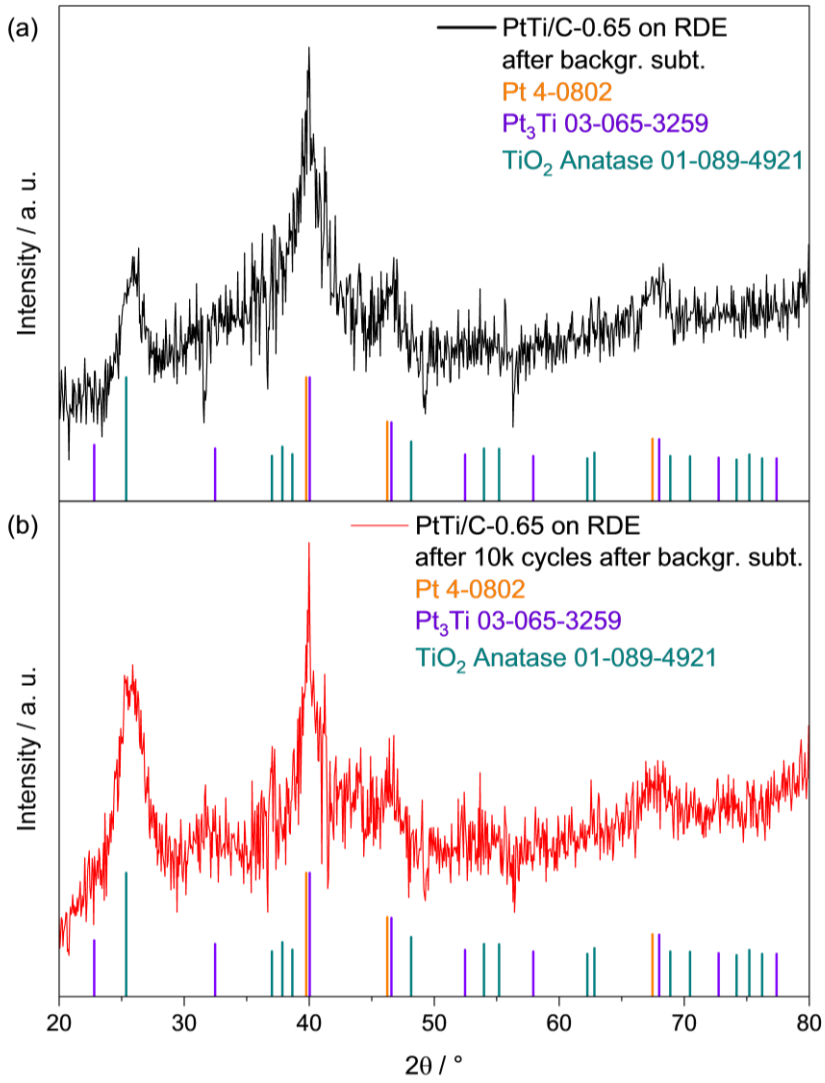

Figure S23. *GIXRD pattern after background subtraction of the RDE pattern of (a) the PtTi/C-0.65 catalyst deposited on the RDE before and (b) after 10,000 cycles AST. The peak at 26.7°2θ can belong to the (002) plane of graphitic carbon from the glassy carbon and the carbon support of the particles and can therefore not be used for analysis.*

26. XPS stability measurements of PtTi/C-0.65 after 10,000 cycles AST

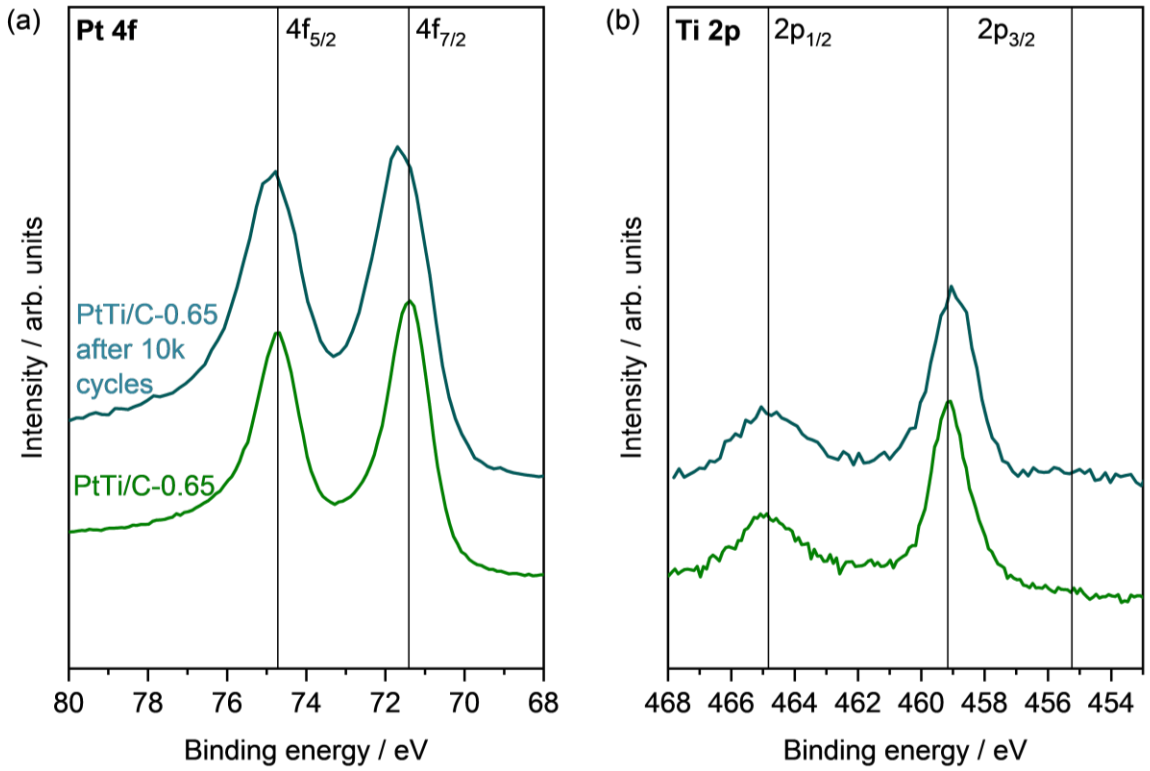

Figure S24. *XPS spectra of PtTi/C-0.65 catalyst before and after 10,000 cycles AST. (a) Pt 4f and (b) Ti 2p XPS spectra.*

27. TEM investigation of PtTi/C-0.65 after 10,000 cycles AST

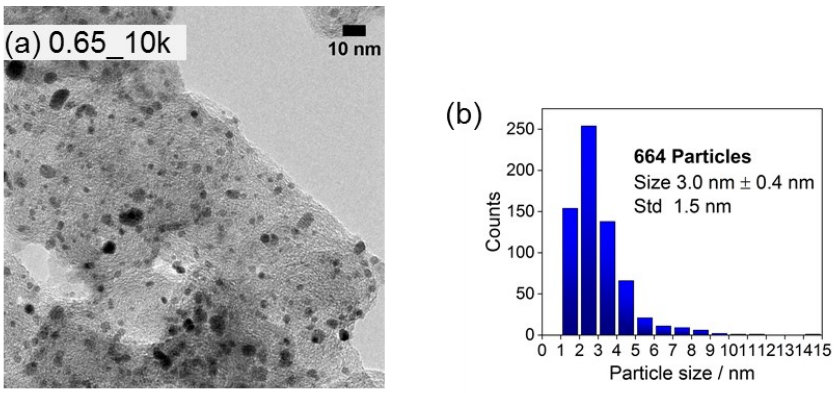

Figure S25. *(a) TEM micrograph of PtTi/C-0.65 after 10,000 voltage cycles AST and (b) corresponding particle size distribution. The average of the particle diameters is given with a calculated error, and the standard deviation (Std) of the mean is noted in addition.*

28. Composition of PtTi/C-0.65 before and after 10,000 cycles AST

Table S7*. PtTi composition before and after electrochemical cycling determined by EDX – the nominal compositional EDX data were corrected by initial actual ICP-OES data of sample.*

Sample	Initial		After 10,000 CVs	
	at% Pt	at% Ti	at% Pt	at% Ti
PtTi/C-0.65-EDX	40	60	53	47
PtTi/C-0.65-corrected	45	55	67	33

References

1. Peng, Z.; Yang, H. *Nano Today* **2009,** 4, (2), 143-164.
2. Massalski, T. B.; Murray, J. L.; Bennett, L. H.; Baker, H., *Binary alloy phase diagrams*. American Society for Metals: Metals Park, Ohio, 1986.